Materials Science Forum Vols. 633-634 (2010) pp 39-53
Online available since 2009/Nov/19 at www.scientific.net

doi:10.4028/www.scientific.net/MSF.633-634.39

A Computational Model for Intergranular Fracture in Nanocrystalline and Ultra-Fine Polycrystalline Metals

Bo Wu[1, 2], Yueguang Wei[1,a]

[1]State-Key Laboratory of Nonlinear Mechanics, Institute of Mechanics, Chinese Academy of Science, Beijing 100190, China

[2]Engine Engineering Center, China North Engine Research Institute, Langfang 065000, China

[a]Ywei@Lnm.imech.ac.cn

Keywords: intergranular fracture; polycrystalline metals; cohesive model; finite element method.

Abstract. By means of finite element method which is based on the conventional theory of mechanism-based strain gradient plasticity, cohesive interface model is used to study the intergranular fracture in polycrystalline metals with nanoscale and ultra-fine grains. A systematical study on the overall strength and ductility of polycrystalline aggregates which depend on both grain interiors and grain boundaries for different grain sizes is performed. The results show that the overall strength and ductility of polycrystalline aggregates with nanoscale and ultra-fine grains are strongly related to the competition of grain boundaries deformation with that in grain interiors. Finally, the deformation and failure behavior of nanocrystalline nickel are described by using the computational model.

Introduction

Mechanical behaviors of polycrystalline metallic materials with grain sizes typically less than 100nm (nanocrystalline (nc) metals) or within 100-1000nm (ultra-fine crystalline (ufc) metals) have undergone the intensely worldwide attention over the past two decades. Relative to bulk case, the nc/ufc metals exhibit high yield stress, tensile strength, and hardness, but the lower tensile ductility. Although the micromechanisms governing the macroscopic mechanical behavior of polycrystalline aggregates were documented [1-3], very few direct experimental evidence exists to show the fracture and failure processes in nc and ufc metals, especially the competition of grain interior and grain boundary inelastic deformation. Recently Shan et al. [4] reported that grain boundary–mediated processes dominate the nc metal deformation through observation for the nc nickel films using the transmission electron microscope (TEM). Moreover, many molecular dynamics (MD) simulations also presented that grain boundary related slip and separation phenomena plays an important role in the overall inelastic response of a polycrystalline material with decreasing the grain-size [5-9]. Due to the limitation of time and dimensional scale in the MD simulations, that is too large computational cost to simulate the mechanical behaviors of the nc/ufc metals with realistic experiment sample sizes, boundary conditions, strain rates and impractical to compare with experimental results, several continuum constitutive methods have been presented to explore the effect of grain boundary in the plastic deformation and failure response of the nc materials [3, 10-16]. Studies using the high-resolution transmission electronic microscopy (HRTEM) show that the nature of intercrystalline grain-boundary regions strongly depends on how the material has been processed. Many grain boundaries appear sharp, well-defined and no distinct grain boundary phases, the others show considerable disorder in grain boundary regions [2, 17]. Considering the inherently characteristic of grain boundaries in the nc/ufc metals, both the grain boundary affected zone (GBAZ) model [3, 11-13] and the traction-separation cohesive interface model [14,15] were proposed to represent the grain boundary response in polycrystalline aggregates.

Despite that the comprehensive computational analyses of the deformation in the nc/ufc materials using above mentioned continuum-level models were carried out recently, it is difficult to unambiguously define the interfacial properties of grain boundaries, and the conventional

elastic-plastic theory is also difficult to characterize the size effects of intragranular inelastic deformation with various grain sizes in nano/ultra-fine grain sizes regime. In the present research, the conventional theory of mechanism-based strain gradient plasticity (CMSG) [18] is used to simulate the strengthening response and size effects of the inelastic deformation in grain interiors, and a cohesive interface model is used to simulate both the grain-boundary separating and the intergranular fracture process. Particular attention is focused on the influence of both grain interiors and grain boundary properties on the overall strength and ductility of the nc/ufc metals. Finally, applications of the model to describe the deformation and failure response of nickel polycrystalline with various grain sizes are carried out.

Constitutive laws and computational model

The CMSG constitutive law for intragranular inelastic deformation. To model intragranular inelastic deformation of polycrystalline aggregates at small scales approaching the nanoscale, due to the grain size effect, the mechanical behaviors of the grain interiors can not well be described by using the classical elastic-plastic theory. So in the present research, the CMSG theory presented by Huang et al [18] will be used. Unlike the general strain gradient plasticity theories[19, 20], the CMSG theory is a lower-order theory which does not involve high-order stresses or additional boundary conditions, and therefore preserves the same theoretical structure as the classical theory except including a partial hardening due to strain gradient effect. Here a brief description of the CMSG constitutive relations and the corresponding finite element analysis are provided as follows.

The CMSG constitutive relations incorporate Taylor dislocation model through the effective strain rate. For small dislocation density, Taylor dislocation model [21-22] gives the shear flow stress in terms of the dislocation density ρ by

$$\tau = a\mu b\sqrt{\rho} = \alpha\mu b\sqrt{\rho_S + \rho_G} \ , \tag{1}$$

where μ is the shear modulus; b is the magnitude of the Burgers vector; α is an empirical coefficient around 0.3 depending on the material structures and characteristic. ρ_S and ρ_G are densities of statistically stored dislocations(SSD) and geometrically necessary dislocations (GND) [23-25], respectively. The former is accumulated by trapping each other in a random way, while the latter is introduced by Nye to ensure the compatibility of the nonuniform plastic deformation. The GND density is related to the effective plastic train gradient η^p by

$$\rho_G = \overline{r}\frac{\eta^p}{b} . \tag{2}$$

where $\overline{r}$ is the Nye-factor to reflect the effect of crystallography on the distribution of GNDs and is around 1.90 for face-centered-cubic (fcc) polycrystals. While η^p is effective plastic strain gradient.

The tensile flow stress σ_{flow} is related to the shear stress τ by

$$\sigma_{flow} = M\tau = M\alpha\mu b\sqrt{\rho_S + \overline{r}\frac{\eta^p}{b}} \ , \tag{3}$$

where M is Taylor factor which acts as an isotropic interpretation of the crystalline anisotropy at the continuum level, and M is about 3.06 for fcc metals [26-28]. Since the effective plastic strain gradient η^p vanishes and flow stress $\sigma_{flow} = \sigma_Y f(\varepsilon^p)$ in uniaxial tension, the SSD density ρ_S is determined from (3) as

$$\rho_{\mathrm{S}} = \left[\frac{\sigma_{\mathrm{Y}} f(\varepsilon^{\mathrm{p}})}{M \alpha \mu b} \right]^2 . \tag{4}$$

Then the flow stress accounting for the nonuniform plastic deformation becomes

$$\sigma_{\mathrm{flow}} = \sqrt{\left[\sigma_{\mathrm{Y}} f(\varepsilon^{\mathrm{p}}) \right]^2 + M^2 \alpha^2 \bar{r} \mu^2 b \eta^{\mathrm{p}}} = \sigma_Y \sqrt{f^2(\varepsilon^{\mathrm{p}}) + l \eta^{\mathrm{p}}} , \tag{5}$$

where

$$l = M^2 \bar{r} \alpha^2 \left(\frac{\mu}{\sigma_{\mathrm{Y}}} \right)^2 b \approx 18 \alpha^2 \left(\frac{\mu}{\sigma_{\mathrm{Y}}} \right)^2 b \tag{6}$$

is the intrinsic material length in strain gradient plasticity, σ_{Y} is the initial yield stress, and f is a non-dimensional function of plastic strain ε^{p} which takes the form

$$f(\varepsilon^{\mathrm{p}}) = \left(1 + \frac{E \varepsilon^{\mathrm{p}}}{\sigma_{\mathrm{Y}}} \right)^N , \tag{7}$$

for a power-law hardening solid, E is the Young's modulus, and N is the plastic work hardening exponent ($0 \le N < 1$).

Huang et al. (2004) [18] demonstrated that the power law visco-plastic model [29, 30] incorporating the strain gradient effects can be applicable to conventional power-law hardening if the rate-sensitivity exponent m is large ($m \ge 20$). Then the plastic strain rate is expressed as

$$\dot{\varepsilon}^{\mathrm{p}} = \dot{\varepsilon} \left[\frac{\sigma_{\mathrm{e}}}{\sigma_{\mathrm{Y}} \sqrt{f^2 \left(\varepsilon^{\mathrm{p}} \right) + l \eta^{\mathrm{p}}}} \right]^m , \tag{8}$$

where $\dot{\varepsilon} = \sqrt{\frac{2}{3} \dot{\varepsilon}'_{ij} \dot{\varepsilon}'_{ij}}$ is the effective strain rate and $\dot{\varepsilon}'_{ij}$ is the deviatoric strain rate.

The constitutive relation in CMSG, which involves the conventional stress and strain only, can be expressed as give the stress-rate $\dot{\sigma}_{ij}$ in terms of the strain-rate as follows

$$\dot{\sigma}_{ij} = K \dot{\varepsilon}_{kk} \delta_{ij} + 2\mu \left[\dot{\varepsilon}'_{ij} - \frac{3\dot{\varepsilon}}{2\sigma_{\mathrm{e}}} \left(\frac{\sigma_{\mathrm{e}}}{\sigma_{\mathrm{flow}}} \right)^m \sigma'_{ij} \right]$$

$$= K \dot{\varepsilon}_{kk} \delta_{ij} + 2\mu \left\{ \dot{\varepsilon}'_{ij} - \frac{3\dot{\varepsilon}}{2\sigma_{\mathrm{e}}} \left[\frac{\sigma_{\mathrm{e}}}{\sigma_{\mathrm{Y}} \sqrt{f^2 \left(\varepsilon^{\mathrm{p}} \right) + l \eta^{\mathrm{p}}}} \right]^m \sigma'_{ij} \right\}, \tag{9}$$

where K is the bulk modulus of elasticity, $\dot{\varepsilon}'_{ij}$ is the deviatoric strain rate, $\sigma_{\mathrm{e}} = \sqrt{\frac{3}{2} \sigma'_{ij} \sigma'_{ij}}$ is the Von Mises effective stress, $\dot{\varepsilon}_{kk}$ is the bulk strain rate, and δ_{ij} is the Kronecker delta tensor. The effective

plastic strain gradient η^{p} in CMSG is define in the same way as that in the higher-order MSG theory [31], and is given by

$$\eta^{\mathrm{p}} = \int \dot{\eta}^{\mathrm{p}} dt \,,\ \dot{\eta}^{\mathrm{p}} = \sqrt{\frac{1}{4}\dot{\eta}^{\mathrm{p}}_{ijk}\dot{\eta}^{\mathrm{p}}_{ijk}} \,,\ \dot{\eta}^{\mathrm{p}}_{ijk} = \dot{\varepsilon}^{\mathrm{p}}_{ik,j} + \dot{\varepsilon}^{\mathrm{p}}_{jk,i} - \dot{\varepsilon}^{\mathrm{p}}_{ij,k} \,, \tag{10}$$

where $\dot{\varepsilon}^{\mathrm{p}}_{ij}$ is the tensor of plastic strain rate. Since the CMSG theory does not involve the higher-order stress, equilibrium equations and traction boundary conditions remain the same as the conventional theories.

Observing (9), since the CMSG theory does not involve the higher-order stress, equilibrium equations and traction boundary conditions remain the same as the conventional theories.

Generally speaking, when the strain gradient effect is considered, the conventional finite element method fails [20]. However the CMSG theory is a lower-order theory which does not involve the higher-order stress such that the governing equations are essentially the same as those in the classical plasticity. One can easily modify the existing finite element program to incorporate the plastic strain gradient effect approximately [32]. In the present research, we have implemented a C^0 three-dimensional solid element incorporating the CMSG theory in the ABAQUS finite element program via its User-Material subroutine UMAT.

Finite element method (FEM) and boundary conditions. To particularly study the mechanical behaviors of the nc/ufc materials, as shown in Fig.1(a), and to investigate how the competition of grain-boundary deformation with that in the grain interiors determines the observed macroscopic stress-strain response and the overall ductility of polycrystalline aggregates by various properties of grain boundaries and grain interiors. A regular quasi-three-dimensional representative volume element with taking into account of three dimensional effects is presented here. Fig.1(b) shows the schematic drawing of representative calculation model. The calculation model is consisted of seven idealized hexagon grains, and the diameter d of grain is the diameter of circumcircle of hexagon. As displayed in Fig.1(b), periodic boundary conditions are enforced along the four sides in y_1y_2 coordinate plane[33]:

$$\overline{\mathbf{u}}_{12} - \overline{\mathbf{u}}_{v_4} = \overline{\mathbf{u}}_{11} - \overline{\mathbf{u}}_{v_1} \tag{11}$$

$$\overline{\mathbf{u}}_{22} - \overline{\mathbf{u}}_{v_1} = \overline{\mathbf{u}}_{21} - \overline{\mathbf{u}}_{v_2} \tag{12}$$

$$\overline{\mathbf{u}}_{v_3} - \overline{\mathbf{u}}_{v_2} = \overline{\mathbf{u}}_{v_4} - \overline{\mathbf{u}}_{v_1} \tag{13}$$

Here, $\overline{\mathbf{u}}_{ij}$ is the displacement vector for any material point on the corresponding boundary Γ_{ij}, and $\overline{\mathbf{u}}_{v_i}$ the displacement vector for each vertex v_i. Rigid body motions can be eliminated by requiring that $\overline{\mathbf{u}}_{v_k} = 0$, for either $k \in \{1,2,4\}$. Otherwise, a displacement boundary condition $\overline{\mathbf{u}}_{\mathrm{Z}}$ which considers the third dimensional effect is enforced in the y_3 coordinate direction perpendicular to y_1y_2 coordinate plane, assuming that the material geometry in z direction is also a periodic structure which has a finite-thickness.

The cohesive interface model used in describing grain boundary fracture. The intergranular fracture process is described by using the cohesive interface model. Cohesive interface model was presented early in the literature of Barenblatt [34] and Dugdale [35] to model fracture more than 40 years ago. In recent years, numerous cohesive interface model formulations have been widely presented and used to simulate fracture initiation and propagation [36-38], and the traction-separation relations of cohesive interface are extended to represent grain boundaries modeling the phenomena of grain-boundary sliding and separation [14, 15, 39]. In the current numerical study, a mixed-mode

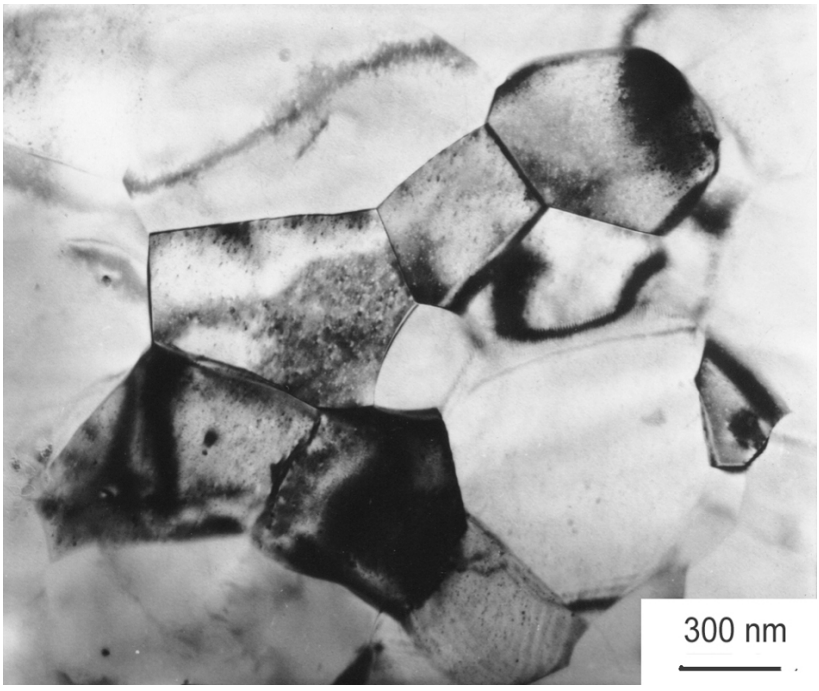

(a)

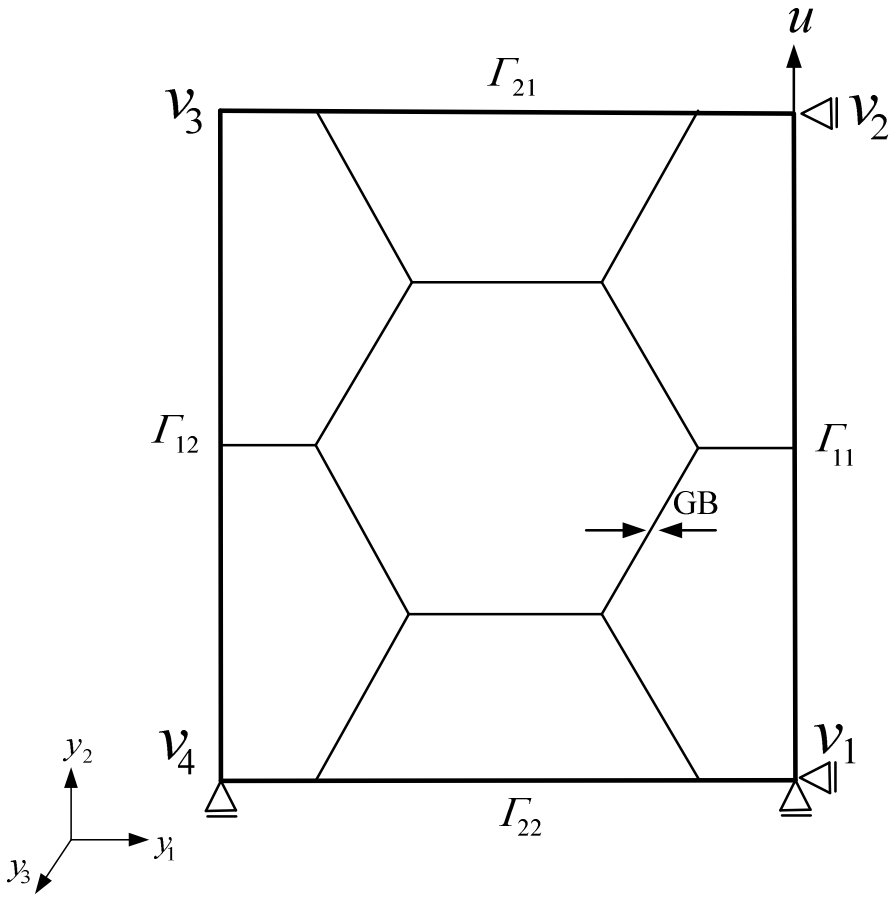

(b)

Fig. 1 (a) A representative cell photo of ultra-fine polycrystalline metal [3]; (b) Computational model and periodic boundary conditions

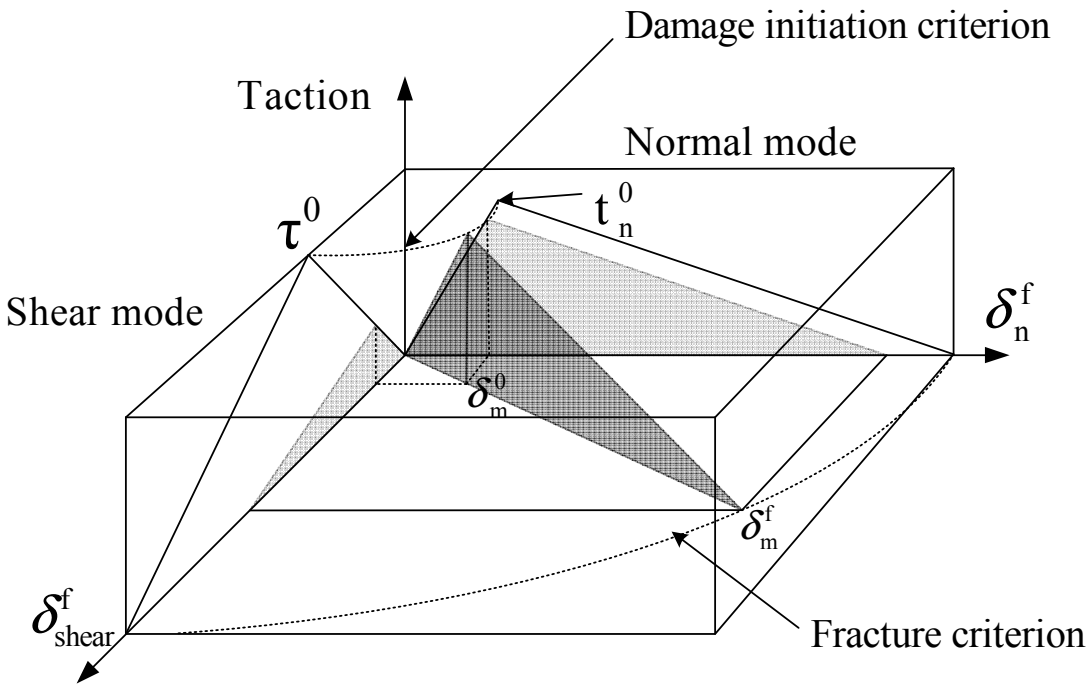

(a)

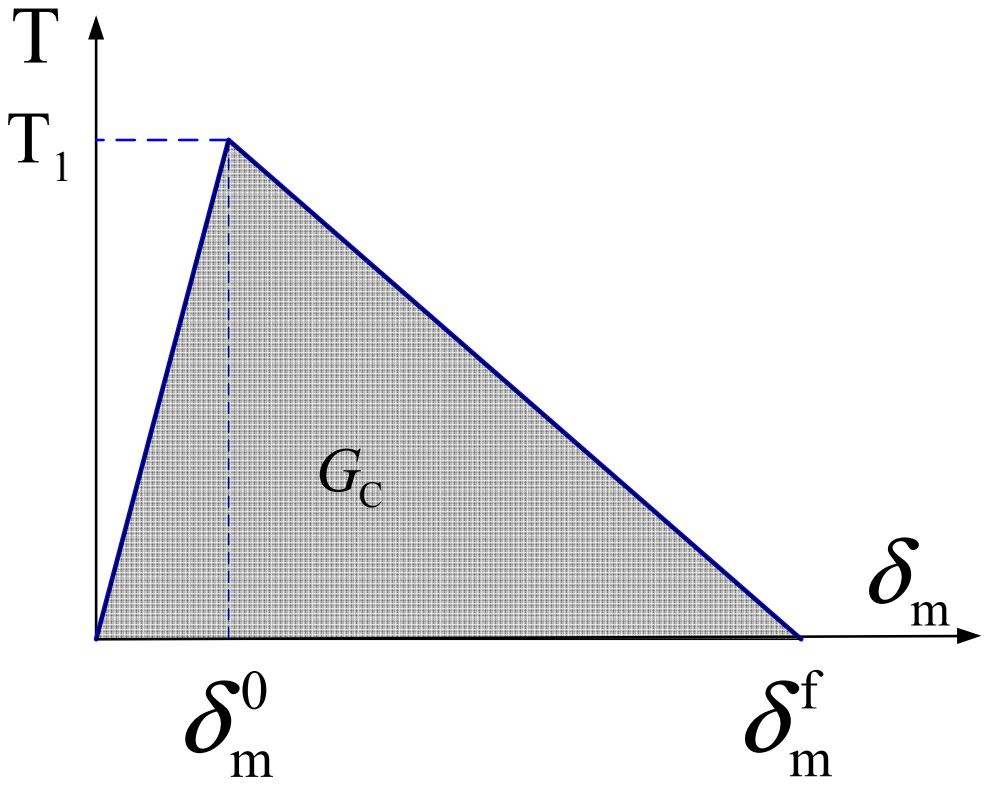

(b)

Fig. 2 (a) Illustration of mixed-mode response in cohesive interface model; (b) Traction-separation relation for a mixed mode loading situation

cohesive interface model developed by Turon et al. [40] has been used to describe the initiation and evolution of intergranular cracks without arbitrarily introducing initial cracks. In which the normal and shear components of traction or displacement across the interface are combined based on a certain mixed mode behavior. The schematic representation of the dependence of damage initiation and

evolution on the mode mix, for a traction-separation response with isotropic shear behavior is shown in Fig.2(a). The figure shows the traction on the vertical axis and the magnitudes of the normal and the shear separations along the two horizontal axes. The unshaded triangles in the two vertical coordinate planes represent the response under pure normal and pure shear deformation, respectively. All intermediate vertical planes (that contain the vertical axis) represent the damage response under mixed mode conditions with different mode mixes. To describe the evolution of damage under a combination of normal and shear deformation across the interface, it is useful to introduce an effective displacement defined as

$$\delta_{\mathrm{m}} = \sqrt{\langle \delta_{\mathrm{n}} \rangle^2 + \delta_{\mathrm{s}}^2 + \delta_{\mathrm{t}}^2} \ . \tag{14}$$

Where the $\langle\ \rangle$ represents the Macaulay bracket, is used to signify that a pure compressive deformation does not initiate damage. δ_{n}, δ_{s} and δ_{t} represent the relative displacements when the deformation is either purely normal to the interface or purely in the first or the second shear direction respectively. The mixed-mode traction-separation relations with a linear damage evolution are illustrated in Fig.2(b). Here T is traction, δ_{m}^0 is the critical separation effective displacement at damage initiation and T_{l} is corresponding critical traction, $\delta_{\mathrm{m}}^{\mathrm{f}}$ is separation effective displacement at complete failure and K_{c} is the initial separation stiffness of cohesive element. As shown in Fig.1(b), the separation process of grain boundaries between two hexagon grains is modeled by using the cohesive interface layers with zero thickness.

Results and discussion

Intergranular fracture affected by intragranular and interfacial material paramters. In this section, the comparative parameter studies of the overall strength and ductility of polycrystalline aggregates affected by the material parameters of grain boundaries and grain interiors with different grain sizes are performed. The overall stress-strain relation with parameter dependence normalized by the intragranular initial yield stress σ_{y} and intrinsic material length l of grain interior can be expressed as follows

$$\frac{\sigma}{\sigma_{\mathrm{y}}} = F\left(\frac{E}{\sigma_{\mathrm{y}}}, \nu, N, \frac{d}{l}; \frac{T}{\sigma_{\mathrm{y}}}, \frac{K_{\mathrm{c}}}{\sigma_{\mathrm{y}}}, \frac{\delta_{\mathrm{m}}^{\mathrm{f}} - \delta_{\mathrm{m}}^0}{l}; \varepsilon\right), \tag{15}$$

where the intragranular material parameters are Young's modulus E, Poisson's ratio ν, initial yield stress σ_{y} and plastic work hardening exponent N respectively. The interfacial parameters of grain boundary are traction T, initial separation stiffness K_{c}, and the effective damage evolution displacement $(\delta_{\mathrm{m}}^{\mathrm{f}} - \delta_{\mathrm{m}}^0)$ of cohesive interface model. Here d is the grain diameter.

The stress-strain curves of polycrystalline aggregates having various intragranular material elastic moduli E with two grain sizes $d = 0.1 l_0$ and $d = l_0$ (Here l_0 is the intrinsic material length of grain interior when the intragranular elastic modulus $E = E_0$) are presented in Fig.3. A clear dependence on the grain sizes and intragranular elastic modulus of overall strength and ductility was observed. As shown in Fig.3, the ultimate tensile stresses of polycrystalline aggregates increase with the intragranular elastic modulus increasing, whereas the global ductility is decreased simultaneously. And this phenomenon is more obvious with the grain size decreasing.

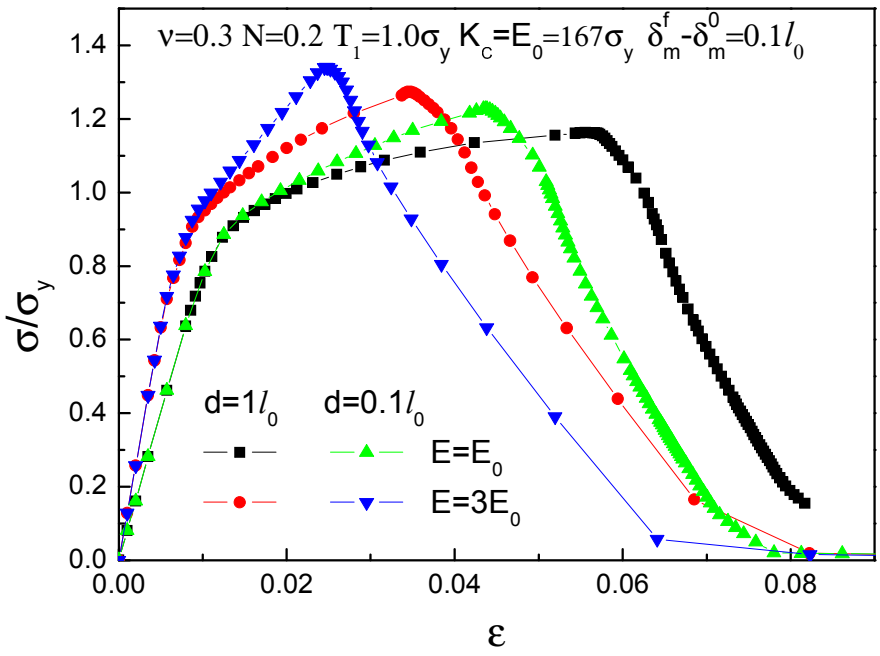

Fig. 3 The dependence of the stress-strain relations on different elastic moduli (E) of grain interior with several grain sizes (d / l_0)

Fig.4 shows the dependence of the stress-strain relations on the intragranular plastic work hardening exponent N for different grain sizes $d = 0.1l$ and $d = l$. From Fig.4, the overall ductility and strength of polycrystalline are sensitive to plastic work hardening exponent. When the exponent N is small, the occurrence of intergranular fracture will be deferred greatly, but the effect of work hardening is not obvious. Furthermore, the grain size effect will be decreased while the grain interiors have bigger plastic work hardening exponent.

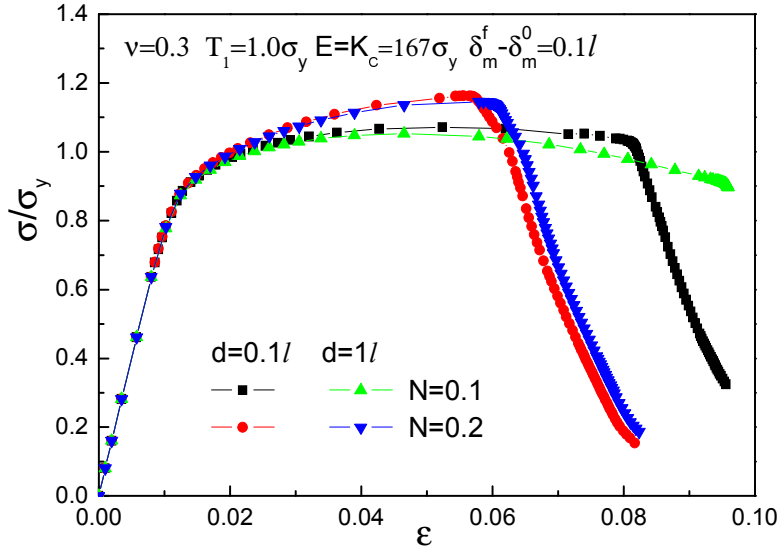

Fig. 4 The dependence of the stress-strain relations on different plastic work hardening exponent (N) of grain interior with several grain sizes (d / l)

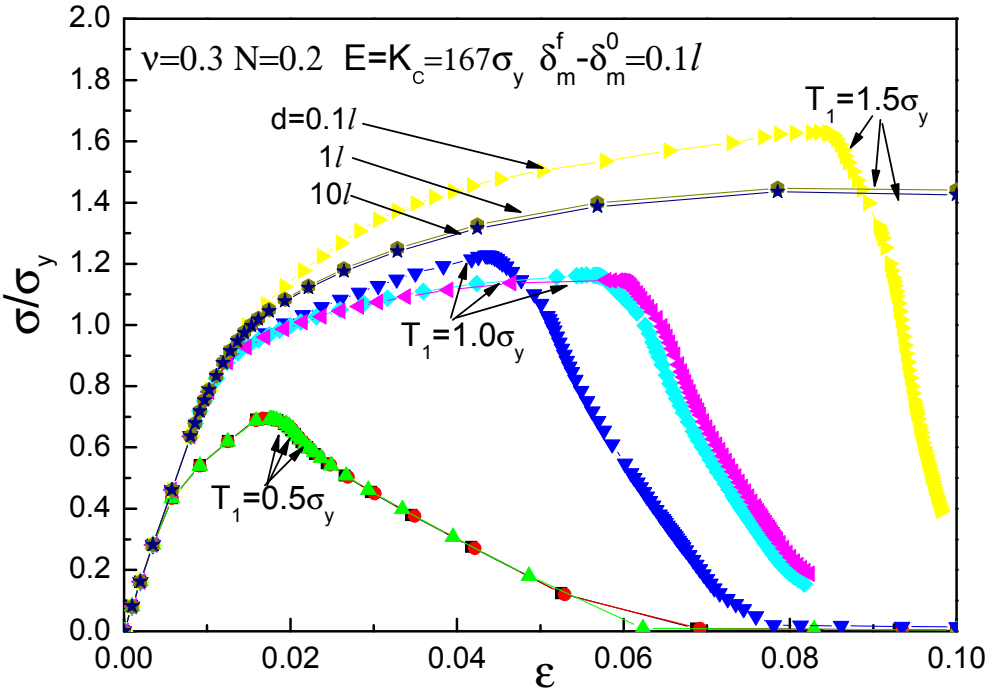

Fig. 5 The dependence of the stress-strain relations on variation ratio (T_1/σ_y) with several grain sizes (d/l_0)

Fig.5 shows the dependence of the stress-strain relations on (T_1/σ_y) with various grain sizes ($d=0.1l, l$ and $10l$). Here (T_1/σ_y) is the ratio of critical separation stress of cohesive interface to initial yield stress of grain interior. The results show that the global strength and ductility of polycrystalline aggregates are very sensitive to the ratio (T_1/σ_y). The macroscopic ultimate tensile strength and ductility of polycrystalline greatly increase when the ratio $T_1/\sigma_y=1.5$ respect to $T_1/\sigma_y=0.5$, while the moderate strength and ductility are shown with $T_1/\sigma_y=1.0$. Additionally the grain size effects in inelastic deformation are more obvious with the value of ratio T_1/σ_y increasing. Furthermore, when the grain diameter $d\geq l$, the dependence of intergranular fracture on the grain size is gradually diminished, such as shown in Fig.5 with $d/l=1.0$ and 10. While the ratio $d/l=0.1$, the grain size effects in plastic flow can be observed obviously. All above means that the ratio T_1/σ_y is a critical control parameter for the competition of grain-boundary deformation with that in the grain interiors to define the global strength and ductility of polycrystalline aggregates. The intragranular elastic-plastic deformation would be dominant and the polycrystalline materials will present good ductility and high strength when $T_1\geq\sigma_y$. Otherwise the grain boundaries related slip and separation phenomena maybe begin to play an important role in the overall inelastic response of a polycrystalline material and a brittle fracture would be appearance for $T_1<\sigma_y$. In the nc/ufc metals, the dislocation-based slip processes in the grain interiors are restrained gradually while the intragranular initial yield stresses are getting higher with decreasing grain sizes. So improving the resistance of grain boundaries to intergranular fracture may be an effective method to improve the bulk properties.

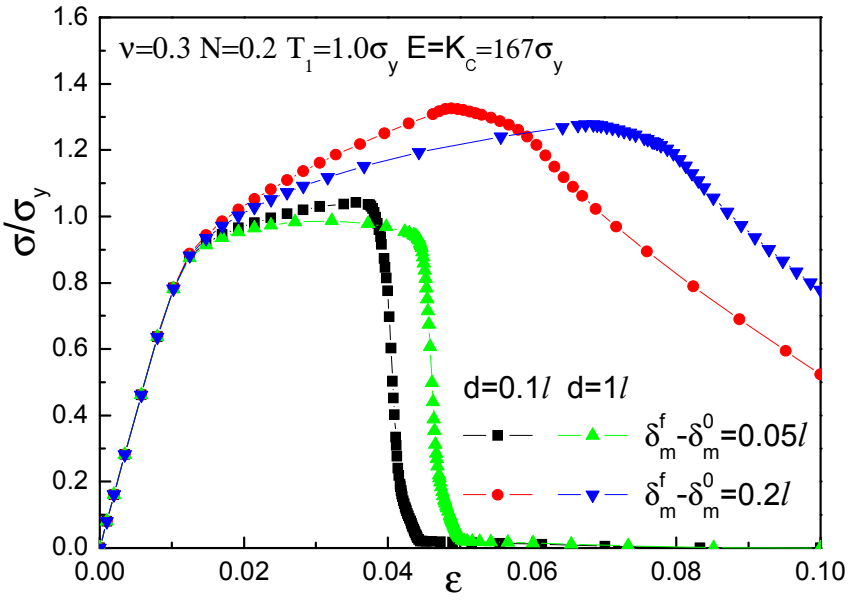

Fig. 6 The dependence of the stress-strain relations on variation of damage evolution range ($\delta_{\mathrm{m}}^{\mathrm{f}} - \delta_{\mathrm{m}}^{0}$) with several grain sizes (d / l)

Fig.6 shows how the variation of damage evolution range ($\delta_{\mathrm{m}}^{\mathrm{f}} - \delta_{\mathrm{m}}^{0}$) of cohesive interfacial model influences the overall mechanical response for a series of grain sizes. From Fig.6, the overall ductility and strength are both increased with increasing the damage evolution range. The contribution to overall ductility decreases with decreasing the grain sizes.

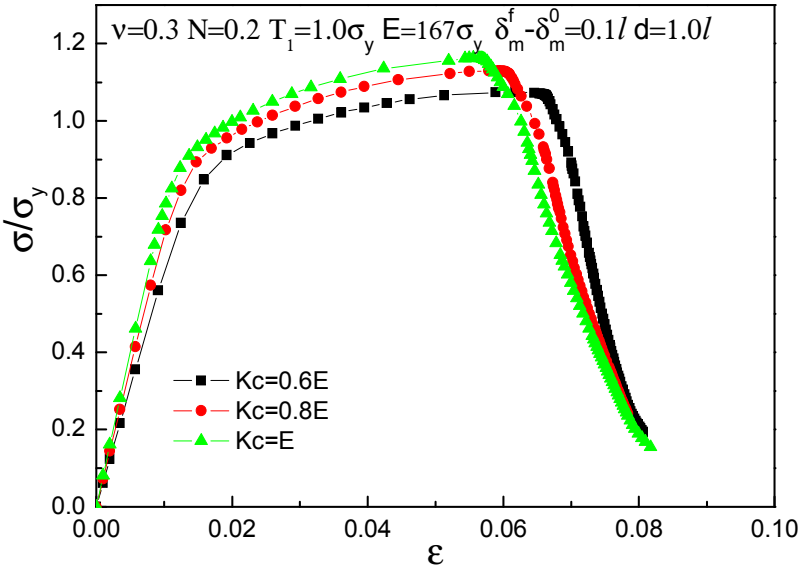

Fig. 7 The dependence of the stress-strain relations on different initial stiffness (K_{C}) with uniform fracture energy release rate (G_{C}) and invariable critical separation stress (T_{1}) of grain boundary

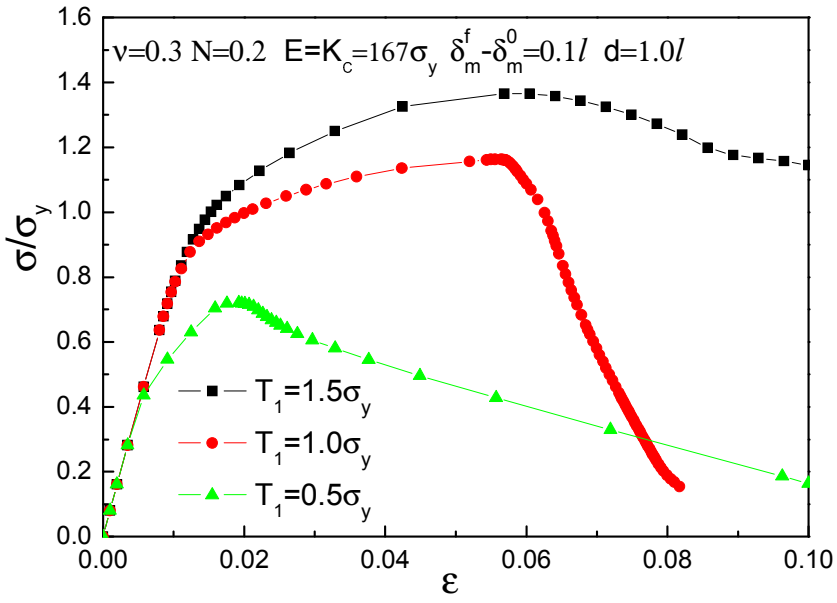

Fig. 8 The dependence of the stress-strain relations on several initial separation stress (T_1) with uniform fracture energy release rate (G_C) and initial stiffness (K_C) of grain boundary

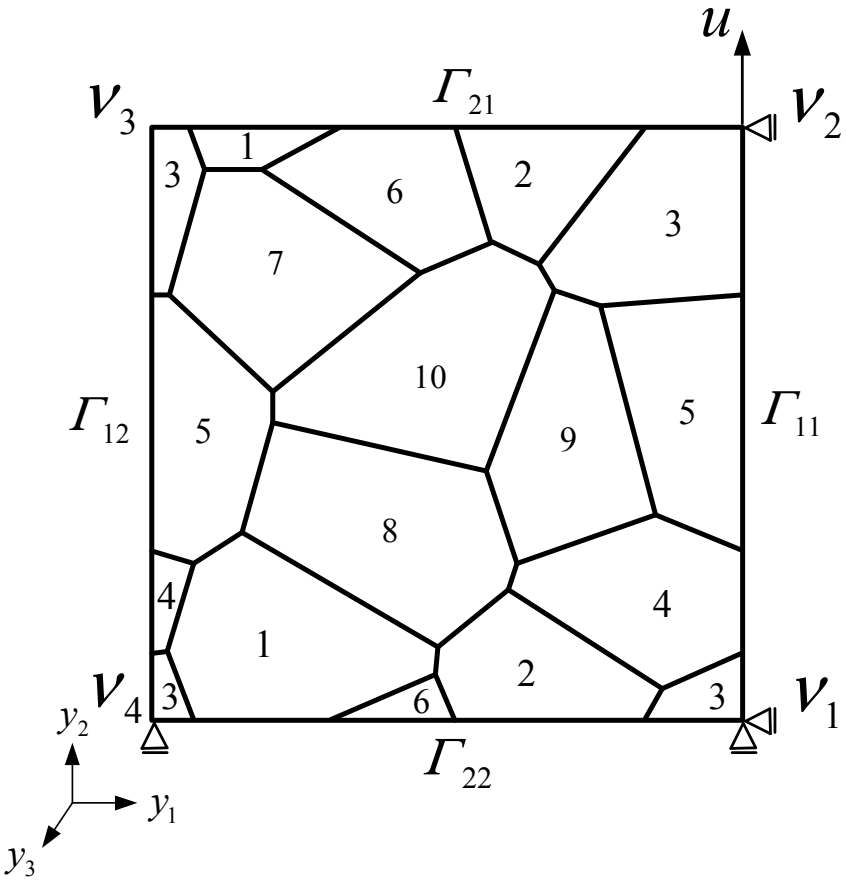

Fig. 9 Schematic drawing of representative calculation model and boundary conditions of polycrystalline aggregates with initial microstructure

In Fig.7 and Fig.8, a uniform energy release rate of grain boundary fracture is considered with initial separation stress T_1 (Fig.7) and initial stiffness (Fig.8) fixed, respectively. The results show that the stress-strain relations are sensitive to the initial separation stress T_1 when the energy release rate of grain boundary fracture is fixed. From Fig.8, the intergranular fracture is greatly delayed with increasing initial separation stress T_1. When the T_1 and energy release rate are fixed, different initial stiffness of grain boundaries hardly influence the strength and ductility (Fig.7).

An application to nanocrystalline nickel. In a realistic physical sample of polycrystalline aggregates there are many factors which are relate to the initiation and propagation of intergranular fracture. The distribution of grain geometry and grain property is also an important factor. However, the geometry topology and material parameters of realistic polycrystalline are too complexity to be confirmed correctly. For the reasons of computational efficiency, a quasi-three-dimensional polycrystalline aggregate model which includes ten polygon grains is constructed by Voronoi tessellation method as shown in Fig.9. Periodic assumption is used to ensure the grain geometry is continuum and material parameters of grain interiors are uniform in the grains of each boundary of the opposite edges pair. Periodic boundary conditions taking into account the three dimensional effects are enforced on the cell mode.

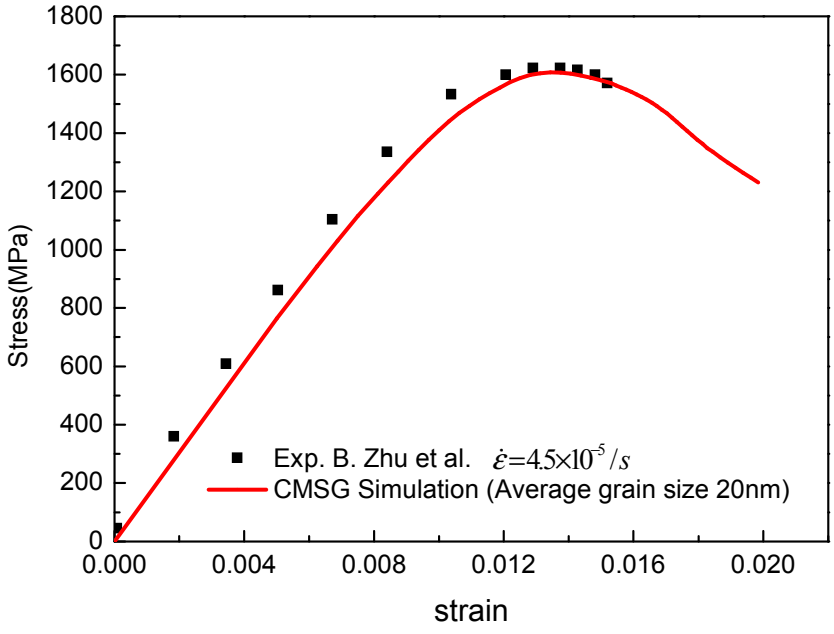

Fig. 10 Comparison of experimental and computational results for uniaxial tension boundary condition with average grain size of 20nm.

Once the geometry of representative cell model is generated, the material parameters of grain interiors and grain boundaries are assigned necessarily. In polycrystalline aggregates, upon being subjected to external tractions, develops a highly inhomogeneous state of internal stresses and additional stresses in the regions adjoining the grain boundaries specially, due to the elastic anisotropy of the individual grains. In the present study, the intragranular properties are allowed to vary from grain to grain but the individual grain is taken to be isotropic with different Young moduli, and parameters of cohesive interfacial model are the same for all grain boundaries in the sample.

The values of the elastic stiffness parameters for FCC metal nickel are taken as [41]

$C_{11}=247\text{GPa}$, $C_{12}=147\text{GPa}$, $C_{44}=125\text{GPa}$.

Thus the value of E of each grain interiors is allowed to vary from the smallest elastic stiffness parameter C_{44} to the biggest C_{11} in the current calculation. When the grain diameter $d \geq d_c$ (d_c is a critical grain size below which the dislocations or partial dislocations dominated intragranular deformation mode are vanished, in nickel metals the value of d_c is about ten nanometers [42]), the initial yield stresses of grain interiors are assumed to satisfy the formula [14]

$$\sigma_y \approx \frac{\mu b}{d}, \tag{16}$$

in which the $\mu = \sqrt{(C_{11} - C_{12}) C_{44} / 2}$ denoting the shear modulus, b is the magnitude of burgers vector, d is the grain diameter. Additional each of the yield stresses is allowed to vary $\pm$50MPa in different grain interiors. The value of plastic work hardening exponent N is allowed to vary from 0.1 to 0.2 in different grain interiors. The critical separation nominal stresses of grain boundaries are assumed to be same with the biggest initial yield stress of grain interiors, and the elastic stiffness parameters are assumed to be the same as the elastic properties for grain interiors. The damage evolution range is specified as several nano-meters. All these material parameters of each grain interiors and grain boundaries are listed in Table1 and Table2.

Table 1. Material parameters of grain interiors in each grain of representative calculation model.

	Grain1	Grain2	Grain3	Grain4	Grain5	Grain6	Grain7	Grain8	Grain9	Grain10
E (GPa)	125	147	247	125	147	247	125	147	247	125
σ_y (MPa)	1150	1200	1250	1200	1250	1150	1250	1150	1200	1150
N	0.1	0.15	0.2	0.1	0.15	0.2	0.1	0.15	0.2	0.1

Table 2. Material parameters of cohesive interface model representing grain boundaries.

T_1	K_c^n	K_c^s	$\delta_{\mathrm{m}}^{\mathrm{f}} - \delta_{\mathrm{m}}^{0}$
1250 (MPa)	247 (GPa)	95 (GPa)	3 (nm)

The comparison between numerical results and experimental data [43] with average grain diameter 20 nm is shown in Fig.10. From Fig.10 the stress-strain curves calculated by finite element method agree well with the experimental data in trend. Although the real failure process in electro-deposited nickel polycrystalline with nano-scale grains is complicated. The computational model can characterize the experimentally observed failure trend to some extent [43-45].

Conclusion remarks

By using both the finite element method based on the CMSG theory and the cohesive interface constitutive relation, we have displayed the micro-scale plastic deformation characteristics in polycrystalline aggregates with nc/ufc grains. A systematically parametrical studies on the overall strength and ductility of polycrystalline aggregates considering both grain interiors and grain boundaries for different grain sizes have been performed. The interaction between intragranular plasticity and grain boundary separation has been investigated.

It is worth noting that in the present research, several assumptions and simplifications are adopted, which should cause the deviation between calculation model result with experimental measurement. Firstly, the calculation model is a quasi-three-dimensional cell model and is assumed periodic structures in both y_1y_2 plane and normal direction (z-direction). Secondly, the distributions of the real grain sizes are very complicated, while in the present calculation model the distributions are assumed

regularly. Thirdly, in the present model, the selections of the input parameters for the grain boundary cohesive model and interiors are difficult to be defined correctly due to lacking of experimental data. Moreover, in order to understand the grain boundary behaviors which are usually characterized by the cohesive constitutive model, more efforts are still needed.

Acknowledgements

The subject is supported by the National Science Foundation of China through Grants Nos 10672163, 10721202, 90816004 and by the Chinese Academy of Science through Grant KJCX-YW-M04.

References

[1] H. Gleiter: Acta Mater. Vol. 48(2000), p.1

[2] K. S. Kumar, H. Van Swygenhoven and S. Suresh: Acta Mater. Vol. 51(2003), p. 5743

[3] Y.G. Wei, S. Shu, Y. Du and C. Zhu. International Journal of Plasticity, Vol.21(2005), p.2089

[4] Zhiwei Shan, E. A. Stach, J. M. K. Wiezorek, J. A. Knapp, D. M. Follstaedt and S. X. Mao: Science. Vol. 305(2004), p. 654

[5] H. Van Swygenhoven and P. M. Derlet: Physical Review B. Vol. 64(2001), p.224105

[6] A. Hasnaoui, H. Van Swygenhoven and P. M. Derlet: Science. Vol. 300(2003), p.1550

[7] J. Schiotz, T. Vegge, D. Di Tolla and K. Jacobsen: Physical Review B. Vol. 60(1999), p. 971

[8] K. J. Von Vliet, S. Tsikata and S. Suresh: Appl Phys Lett. Vol. 83(2003), p. 1441

[9] A. Cao and Y.G. Wei. Physical Review B, Vol.76(2007), 024113

[10] Y. Wei, X. Wang and M. Zhao. Journal of Materials Research, Vol.19(2004), p.208

[11] H.-H. Fu, D. Benson and M.A. Meyers, Acta Materialia. Vol. 52(2004), p. 4413

[12] R. Schwaiger, B. Moser, M. Dao, N. Chollacoop and S. Suresh: Acta Materialia. Vol. 51(2003), p. 5159

[13] Y. Wei, X. Chen, S. Shu and C. Zhu,C. Int. J. Mult. Comp. Eng., Vol.4(2006), p.183

[14] Y. J. Wei and L. Anand: J Mech Phys Solids. Vol. 52(2004), p. 2587

[15] D. H. Warner, F. Sansoz and J. F. Molinari: Int. J. Plasticity. Vol. 22(2006), p.754

[16] I.A. Ovid'ko, J. Mater. Sci. Vol. 42(2007), p.1694

[17] S. Ranganathan, R, Divakar and V. S. Ragunathan: Scripta Mater. Vol. 44(2001), p. 1169

[18] Y. Huang, S. Qu, K. C. Hwang, M. Li and H. Gao: Inter. J. Plast. Vol. 20(2004), p. 753

[19] Y. Wei and J.W. Hutchinson. Journal of Mech. Phys. Solids，Vol.45(1997)，p.1253

[20] Y.G. Wei. Eur. J. Mech. A/Solids, Vol.25(2006), p.897

[21].G.I. Taylor: P. Roy. Soc. Lond. A. Vol. 145 (1934), p. 362

[22] J.E. Bailey and P.B. Hirsch: Philos. Mag. Vol. 5(1960), p. 485

[23] M.F. Ashby: Philos. Mag. Vol. 21(1970), p. 399

[24] J. Ney: Acta Metall. Mater. Vol. 1(1953), p. 153

[25] A. Arsenlis and D.M. Parks: Acta Mater. Vol. 47(1999), p. 1597

[26] J.F.W. Bishop and R. Hill: Philos. Mag. Vol. 42(1951), p. 414

[27] J.F.W. Bishop and R. Hill: Philos. Mag. Vol. 42(1951), p. 1298

[28] U.F. Kocks: Met. Trans. Vol. 1(1970), p. 1121

[29] J.W. Hutchinson: Proc. Royal Soc. London A. Vol. 348(1976), p. 101

[30] S. Kok, A.J. Beaudoin and D.A. Tortorelli, Int. J. Plasticity. Vol. 18(2002), p. 715

[31] H. Gao, Y. Huang and W.D. Nix: J. Mech. Physics Solids. Vol. 47(1999), p. 1239

[32] S. Qu, Y. Huang, H. Jiang, C. Liu, P.D. Wu and K.C. Hwang: Int. J. Fracture. Vol. 129(2004), p. 199

[33] O. Van der Sluis, P. J. G. Schreurs and H. E. H. Meijer: Mechanics of Materials. Vol. 33(2001), p. 499

[34] G. I. Barenblatt: Appl. Math. Mech. (PMM). Vol. 23(1959), p. 622

[35] D. S. Dugdale: J. Mech. Physics Solids. Vol. 8(1960), p. 100

[36] A. Needleman: J. Mech. Physics Solids. Vol. 38(1990), p. 289

[37] V. Tvergaard and J. W. Hutchinson: J. Mech. Physics Solids. Vol. 40(1992), p. 1377

[38] Y. Wei and J.W. Hutchinson. Journal of Mech. Phys. Solids，Vol.45(1997)，p.1137

[39] E. Iesulauro, A. R. Ingraffea, S. Arwade and P. A. Wawrzynek: Fatigue and Fracture Mech. Vol. 33(2002), p. 1417

[40] A. Turon, P. Camanho, J. Costa and C. Davila: NASA/TM-2004-213277.

[41] G. Simmons and H. Wang: Single crystal elastic constants and calculated aggregate properties. The MIT press, Cambridge(2001)

[42] N. Wang, Z. R. Wang, K. T. Aust and U. Erb: Acta metal. Mater. Vol. 43(1995), p. 519

[43] B. Zhu, R. J. Asaro, P. Krysl and R. Baoley: Acta Materialia. Vol. 53(2005), p. 4825

[44] H. Li and F. Ebrahimi: Appl. Phys. Lett. Vol. 84(2004), p.4307

[45] H. Li and F. Ebrahimi: Adv. Mater. Vol. 17(2005), p.1969

Ductility of Bulk Nanostructured Materials
10.4028/www.scientific.net/MSF.633-634

A Computational Model for Intergranular Fracture in Nanocrystalline and Ultra-Fine Polycrystalline Metals
10.4028/www.scientific.net/MSF.633-634.39

DOI References
[12] R. Schwaiger, B. Moser, M. Dao, N. Chollacoop and S. Suresh: Acta Materialia. Vol. 51(2003), p. 5159 doi:10.1016/S1359-6454(03)00365-3
[32] S. Qu, Y. Huang, H. Jiang, C. Liu, P.D. Wu and K.C. Hwang: Int. J. Fracture. Vol. 129(2004), p. 199 doi:10.1023/B:FRAC.0000047786.40200.f8
[33] O. Van der Sluis, P. J. G. Schreurs and H. E. H. Meijer: Mechanics of Materials. Vol. 33(2001), p. 499 doi:10.1016/S0167-6636(01)00066-7